Desalination and Water Treatment
www.deswater.com

doi: 10.5004/dwt.2023.30108

315 (2023) 650–662
December

Hazard assessment of debris flow by using FLO-2D and hazard matrix: a case study of Qingshui Gully in the southern Gansu Province, China

Peng Zhang[a], Xingrong Liu[b], Heping Shu[a,c,d,*]

[a]*Hubei Key Laboratory of Disaster Prevention and Mitigation (China Three Gorges University), Yichang 443002, China, email: shuhp@gsau.edu.cn (H. Shu)*
[b]*Geological Hazards Prevention Institute, Gansu Academy of Sciences, Lanzhou 730000, China*
[c]*College of Water Conservancy and Hydropower Engineering, Gansu Agricultural University, Lanzhou 730070, China*
[d]*MOE Key Laboratory of Mechanics on Disaster and Environment in Western China, College of Civil Engineering and Mechanics, Lanzhou University, Lanzhou 730000, China*

Received 5 May 2023; Accepted 18 September 2023

ABSTRACT

Debris flow frequently occurs in high mountains, particularly in dry hot river valleys, and cause severe loss of life and property. The Qingshui Gully of Gansu Province, China was selected as study area. Remote sensing interpretation technology, field investigation, matrix method, and FLO-2D model were applied to obtain distribution of landslides and model parameters, and simulate debris flow depth, velocity, and impact force under different rainfall return periods, and then divide debris flow intensity and hazard. The results indicated an increase in landslides with increasing human activities. The flow depth generally increased from the middle-up stream to downstream when the rainfall return periods ranged from 10 to 100 years, along with a decrease in velocity and impact force from the middle-up stream to downstream. The simulation resulted in a threatened range generally consistent with the actual result of the debris-flow history disaster. The spatial distribution of intensity classes was similar rainfall return periods was ranging from 10 to 100 years. Furthermore, the high-medium intensity area was primarily distributed in the middle-up stream of the study area, whereas the low-intensity area was located downstream. Additionally, the middle-up watershed channel area mostly belonged to the high hazard class, and it existed in the Beiyu River and around the residential area. The low-hazard area was situated downstream of the channel. The medium hazard class was located between the high and low classes. These proportions of low, medium, and high hazard areas were 28.99%, 35.48%, and 35.53% of the total area, respectively. Therefore, the present study provides a reference for fine risk management and disaster warning in dry hot river valleys.

Keywords: Debris flow; Intensity; Hazard; FLO-2D; Qingshui Gully

1. Introduction

Debris flows frequently occur in high mountains and cause severe loss of life and property, in the form of destruction of houses, roads, and railways in urban and rural areas [1–3]. Additionally, extreme climate events and human activities have become increasingly frequent in mountains [4,5], leading to an even higher frequency of debris flow disasters [6,7]. For example, devastating debris flow disasters occurred on August 8, 2010, in Zhouqu County, China, and killed more than 1,700 people [8–10]. Therefore, it is imperative to obtain a threatened range and hazard to prevent and mitigate potential debris flows [11–13].

Debris flows have caused damage principally through deposition, impact, and erosion and can destroy buildings or

* Corresponding author.

infrastructure [14–16]. To obtain the impact range of debris flow damage modes, several researchers have analyzed debris flow initiation, movement characteristics, hazards, and mechanisms, and a series of achievements have been presented [17–20].

Hazards are a crucial part of debris flow research, because they include debris flow frequency (i.e., different rainfall return periods), intensity, and location. Debris flow frequency and intensity can be combined by using the matrix method [11,12,21]. The intensity and location were presented by using different debris flow characteristics, such as flow depth, velocity, impact force, and discharge, and these characteristics are generally correlated with debris flow initiation, movement processes, and mechanisms [22–24].

Subsequently, field observation stations have been built to obtain debris flow characteristics (i.e., depth, velocity, and threatened range), such as in the Jiangjia Ravine station in China [25] and the III Graben Torrent station in Switzerland [26]. This method can directly and rapidly acquire debris flow depth and velocity. However, the number of observation stations was relatively low, and they were mostly distributed on high-frequency debris flow disaster sites; the other sites were lacking [27].

Afterwards, a physical model was developed to simulate debris flow characteristics; therefore, the flume test has been widely applied under various conditions [28,29]. Nevertheless, the flume test cannot accurately reflect natural debris flow characteristics because this method was used based on the similarity principle, and part of intrinsic factors of debris flow may be lacking [30,31].

With respect to the numerical model, it can simulate one or a region of debris flow characteristics after the parameters have been calibrated under different scenarios. The simulation results can be directly applied to assess debris flow intensity and hazard, and the result of hazard can be quantified [30,32]. Numerous numerical models have been successfully developed for debris flow analysis, such as FLO-2D [33], DAN3D [34], and Debris Intermixing [35]. The FLO-2D model has been widely used under different conditions, such as in the threatened range of debris flow, debris flow movement characteristics (i.e., velocity and depth), and debris flow initiation [36]. This model was successfully carried out in the Yosemite Valley, California, USA [37]. After the parameters of the FLO-2D model were calibrated, the historical debris flow disaster event was reproduced, and the debris flow hazard was divided based on the different simulation results. Zhang et al. [36] utilized the FLO-2D model to obtain the deposition, velocity, impact force, and influence zone in the Hanlin Gully of southern Gansu Province, China, and their results were consistent with the measured results from the documented debris flow. Additionally, several researchers observed that the FLO-2D model in debris flow simulation was more reasonable compared with other models under actual case applications [38,39]. These results demonstrate that the FLO-2D model is an effective tool to quantify the debris flow threat range and hazard.

In this study, remote sensing interpretation technology, field investigation, and indoor tests were carried out to obtain distribution of landslides and FLO-2D model parameters. The FLO-2D model was used to simulate debris flow depth, velocity, and impact force under different rainfall return periods (RRP) after the parameters were calibrated. The accuracy and reliability of the simulation results were validated by using debris flow history disasters. The intensity was marked based on the simulation results and criteria of intensity. Further, the debris flow hazard was calculated by applying the matrix method. This study can provide a reference for fine risk management and disaster warning in dry hot river valleys.

2. Study area

The Qingshui Gully is distributed on the northwest of China and south of Lanzhou City, and it is a first tributary of the Beiyu River and a second tributary of the Bailong River (Fig. 1), with Longnan City located nearby. The area of Qingshui Gully is 2.2 km^2, its main channel is 2.4 km long, and the relative elevation difference is more than 1,000 m in the gully, and the slope of the main channel is 47.6%. There are several residential sites in the Qingshui Gully, particularly on both sides downstream.

The study area is a boundary between the subtropical and warm temperate zones, with mean annual temperature and mean annual precipitation of 13°C and 487 mm, respectively [24,40]. Rainfall mostly occurs between May and September, with a proportion of approximately 70%, and it is predominantly in the form of summer rainstorms or continuous rainfall [41], which can provide advantageous rainfall conditions for the occurrence of landslides or debris flow.

The area is located on the Qinghai–Tibet tectonic belt and Wudu arc structure, influenced by the uplift of the Qinghai–Tibet Plateau, and is particularly affected by neotectonics activity [42]. Fracture folds and rock extrusion are common phenomena, and it can lead to broken strata suffering from intense weathering. In contrast, strong earthquake activity frequently was occurred in the Bailong River, and therefore, collapses and landslides are rapidly increasing in the study area. These phenomena offer abundant material conditions for the occurrence of debris flows.

3. Methods

3.1. Remote sensing interpretation and field investigation

To further analyze the change of loose materials for the study area in recent years, different periods of remote sensing images (source of background images from Google Earth) were collected along with field investigations. The results indicated that landslides were mostly distributed on both sides of the middle channel in 2010 (Fig. 2a). With respect to 2019, landslides occurred downstream and upstream of the channel; therefore, the landslides in the downstream area were triggered by human activities, such as road and railway construction, particularly on the village road building. This will eventually damage the soil structure due to limitations of terrain (Fig. 2b), so that abundant materials occurred (Fig. 3a and b). In the upstream area, owing to the long-term water erosion at the foot of the slope, several landslides developed on both sides of the gully (Figs. 2b and 3c). However, there are a series of phyllite rocks in the study area (Fig. 3d) that are

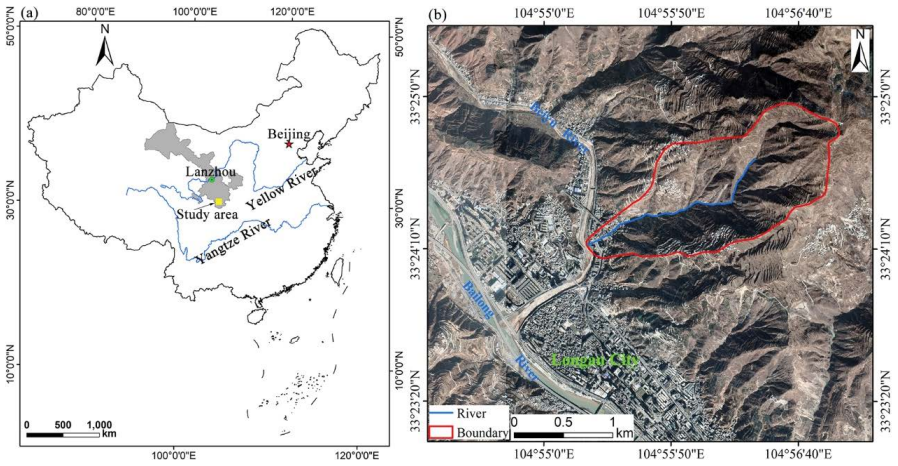

Fig. 1. (a) Geographic position of the study area, (b) remote sensing image of Qingshui Gully. Note: source of background image from Google Earth (https://earth.google.com/web/), dated 2021.

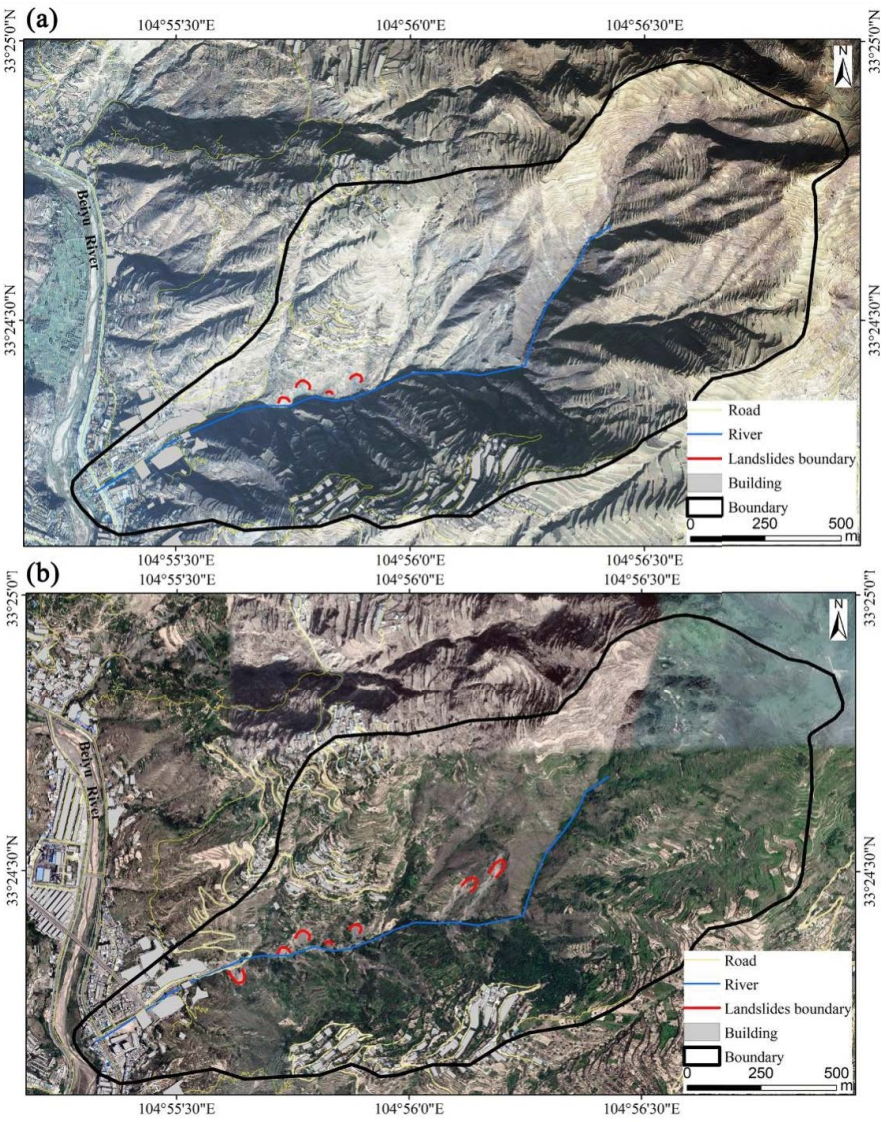

Fig. 2. Distribution of landslides and human activities (i.e., road construction) in different years: (a) 2010 and (b) 2019.

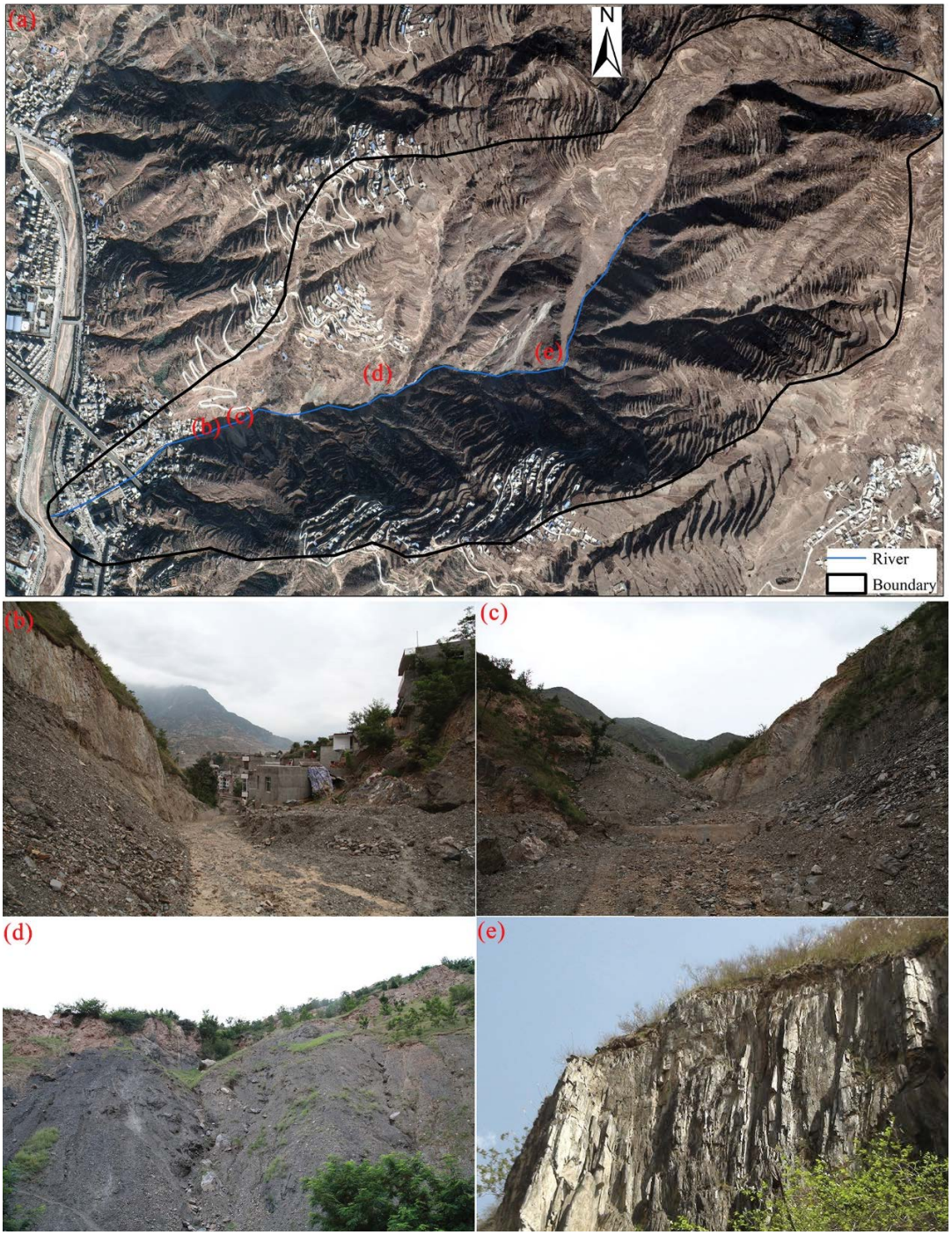

Fig. 3. Material distribution of in the study area: (a) remote sensing image of study area, (b,c) loose materials were triggered due to anthropogenic activities, such as road construction, (d) loose materials provided by natural conditional action, and (e) phyllite rock.

effortlessly weathered under the action of rainfall and wind. Additionally, vegetation on both sides of the channel was sparse, and soil erosion was relatively conspicuous in the study area [24,40]. Under the influence of heavy or continuous rainfall, a debris flow disaster may occur soon. Even if the debris flows loose deposits blocks the channel, and a barrier lake is formed, it will endanger Longnan City.

3.2. Numerical model

3.2.1. FLO-2D model

FLO-2D is a two-dimensional hydraulic model based on volume conservation, and it can be applied to simulate debris flow, mudflow, flood and so on. The velocity, flow depth and impact force were simulated [35,43,44).

The specific content of governing continuity and momentum equation are presented on the O'Brien et al. [33,43]. The hydrodynamic processes of deposition of debris flow movement can be implemented by the FLO-2D numerical model. Moreover, this software has been widely used to simulate the movement characteristics (i.e., flow depth and velocity) of debris flow [45,46]. The simulation results were further applied to assess the intensity and hazard of debris flow. Therefore, the FLO-2D model was applied to simulate the single-channel debris flow disaster movement in the study area under different rainfall return periods, and the simulation results included flow depth, velocity, and impact force.

3.2.2. Numerical model parameter adjustment

The law of regional debris flow disaster occurrence can be found based on historical geohazard data. The results indicate that a relatively large debris flow disaster will occur every 5 years in the study area [24,36,47], such as on August 12, 2010. To adjust the parameters of the numerical model, field investigations, field sampling and indoor tests were conducted after debris flow disasters.

3.2.2.1. Debris flow density

Debris flows generally occur between July and September each year. Therefore, we have set a series of sampling points ranged from upstream to downstream; thereafter, the moisture content was determined by oven-drying the samples for 12 h at 110°C, and the debris flow density can be calculated, with an average density of 1,900 kg/m^3. The grain diameter analysis was performed at the Key Laboratory of Western China's Environmental Systems at Lanzhou University, and the results are presented in Fig. 4. The accumulative proportion was more than 70% when the grain diameter was less than 10 mm, indicating that loose material was relatively easily carried under heavy rainfall or continuous rainfall.

3.2.2.2. Digital terrain model

Topography is represented as a digital code in the process of numerical simulation, and it is the key basic data. The resolution of the digital elevation was 10 m. The irregular triangular mesh model with optimization TIN was established using the ArcGIS software. Meanwhile, the elevation scatter points were collected, and thereafter, the ASCII format was obtained. Finally, this data was used as an input into the FLO-2D PRO software platform to further analyze and calculate the results. Our previous works [36,48,49] instructed that 10 m resolution of digital terrain model (DEM) can be applied to simulate debris flow depth, velocity and impact force in small watershed.

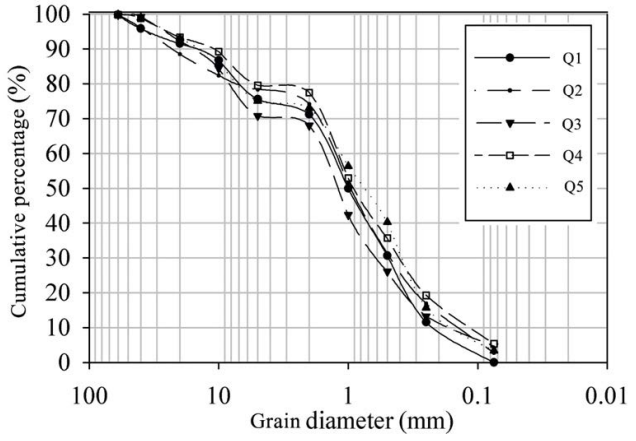

Fig. 4. Grain diameter analysis curve (Q1-Q5 was represented for different sampling points.)

3.2.2.3. Manning coefficient

Manning coefficient was represented for the surface roughness, and it is considered to be an important parameter for numerical model. The manning coefficient was acquired based on the manual of FLO-2D parameter, field investigation, and previous achievements [24,36,49]. The parameter result was 0.15.

3.2.2.4. Sediment volume concentration

In the model, the sediment volume concentration (Cv) was 65%, based on the regional characteristics of rock and soil, results of grain diameter, and previous achievements [36,48]. In addition, the parameter was fine-tuned according to the rationality and reliability of the simulation results in the simulation process.

3.2.2.5. Laminar flow resistance coefficient

The laminar retardation coefficient (K) was set based on the study of Woolhiser [50], Subsequently, it was combined with field investigation and analysis results pertaining to land cover, and the value of K was 2 280.

3.2.2.6. Water flow process line

The P-III method was used to obtain different probabilities of rainfall under different rainfall periods based on historical daily rainfall data [51]. The historical rainfall data ranged from 1951 to 2020, and the different rainfall period values were calculated according to the law formula. The specific results are shown in Table 1.

The extreme rainfall values were 54.2, 60.4, 68.1, and 73.5 mm with return periods of 10, 20, 50, and 100 years, respectively. The rainfall–runoff model was further applied to generate cumulative hydrographs for time between 0 and 24 h [24,48,49] under different rainfall periods (Fig. 5). Cumulative discharge generally increases with increasing rainfall and time.

Table 1
Rainfall intensity under different return period and probability

Name	Data			
Rainfall return period (a)	100	50	20	10
Probability p (%)	1	2	5	10
Rainfall value (mm/d)	73.5	68.1	60.4	54.2

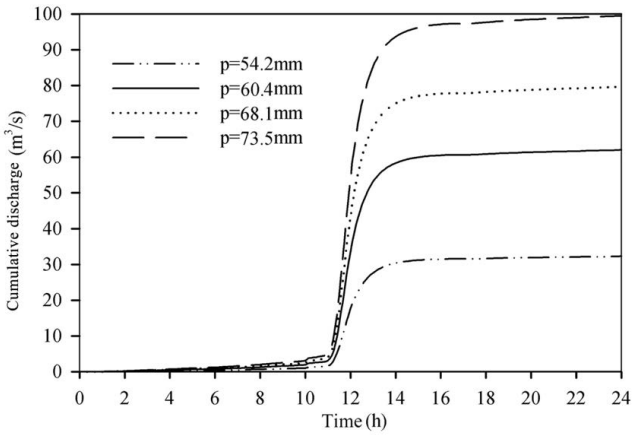

Fig. 5. Cumulative discharge process line under different rainfall by simulating rainfall–runoff module.

3.3. Simulation results validation

Debris flow disasters frequently occur in the study area; hence, the FLO-2D model was used to simulate the characteristics (i.e., flow depth and velocity) of debris flow under different rainfall periods, so that the threat range can be obtained. The reality threat range of debris flow disaster was measured by remote sensing technology, field investigation and questionnaire of local residents on August 12, 2010, and this result was compared with the results of the numerical model.

3.4. Hazard assessment

3.4.1. Intensity assessment

The intensity may be assessed as the spatial distribution, and it may include the distribution of flow depth, velocity, and impact force in this study based on previous achievements [11,52]. Additionally, intensity is required as a part of hazard assessment. The flow depth, velocity, and impact force were selected as quantitative indices to determine the intensity classes based on the results of the numerical simulation. The division criteria of the different indices were based on previous achievements [24,53–55] and the actual situation of the study area. The specific criteria used are listed in Table 2.

3.4.2. Hazard assessment

A hazard can be defined as the probability of occurrence under a specific period and in a given area with a potentially damaging phenomenon [56]. Hazard can be combined by the probability of occurrence and intensity of the process; therefore, intensity is commonly represented as the potential energy (e.g., velocity or flow depth can be selected as the energy index) of flow to the obstacles; probability was presented by different rainfall periods in this study. Generally, probability and intensity are correlated through a hazard matrix [11,16,24,49,57]. The matrix method is simple and easy to apply. The hazard was divided into three classes (low, medium, and high) using ArcGIS software (Table 3).

Table 2
Division criteria of intensity index

Intensity classes	Flow depth (m)	Flow velocity (m/s)	Impact force (kN)
High	>1.0	>3.0	>100,000
Medium	0.5–1.0	1.0–3.0	10,000–1,000,000
Low	<0.5	<1.0	<10,000

Table 3
Hazard assessment matrix used in the approach based on the combination of probability and intensity

Intensity \ Probability	1%	2%	5%	10%
Low	Low	Low	Low	Medium
Medium	Low	Low	Medium	High
High	Medium	Medium	High	High

4. Results and discussion

4.1. Comparison and verification of simulation results

The rainfall amounted to 52.7 mm on the event of debris flow disaster on August 12, 2010 based on the local meteorological station data, and this value was equal to the value of RRP with 10 years. Thereafter, the actual threatened range was determined by remote sensing technology, field investigation and questionnaire of local residents about "8.12" disasters [49], and is presented in Fig. 6 with the threatened range outline marked in red. Additionally, the threatened range appears in Fig. 6 through the numerical simulation, marked in yellow. The threat range of the simulation result was generally consistent with the actual results, and this phenomenon demonstrated that the results of the numerical simulation were very reliable.

4.2. Results of numerical simulation

The parameters of the numerical model were adjusted using remote sensing interpretation, field investigations, indoor tests, and statistical analysis methods. The total length of the watershed was 2.4 km. Meanwhile, the DEM of the study area was divided into 10 m × 10 m grids, with number of grids amounting to 29,327. Subsequently, the debris flow characteristics of the middle and downstream channel sections were simulated by the FLO-2D model in this study, including the flow depth (Fig. 7), velocity (Fig. 8), and impact force (Fig. 9) under different rainfall return periods. In addition, the maximum values of the different characteristics were determined (Table 4).

4.2.1. Flow depth

The distribution of flow depth is presented in Fig. 7 with a RRP of 10, 20, 50, and 100 years. In addition, the flow depth generally increased from the middle-up stream to the downstream (Fig. 7). The flow depth was low when the velocity

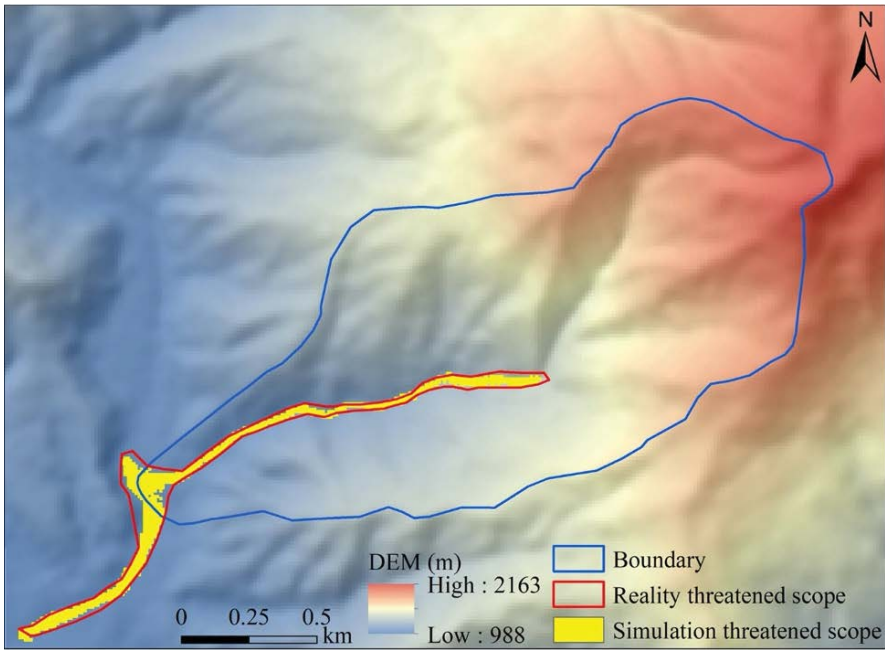

Fig. 6. Comparison of actual hazard area to simulation hazard area.

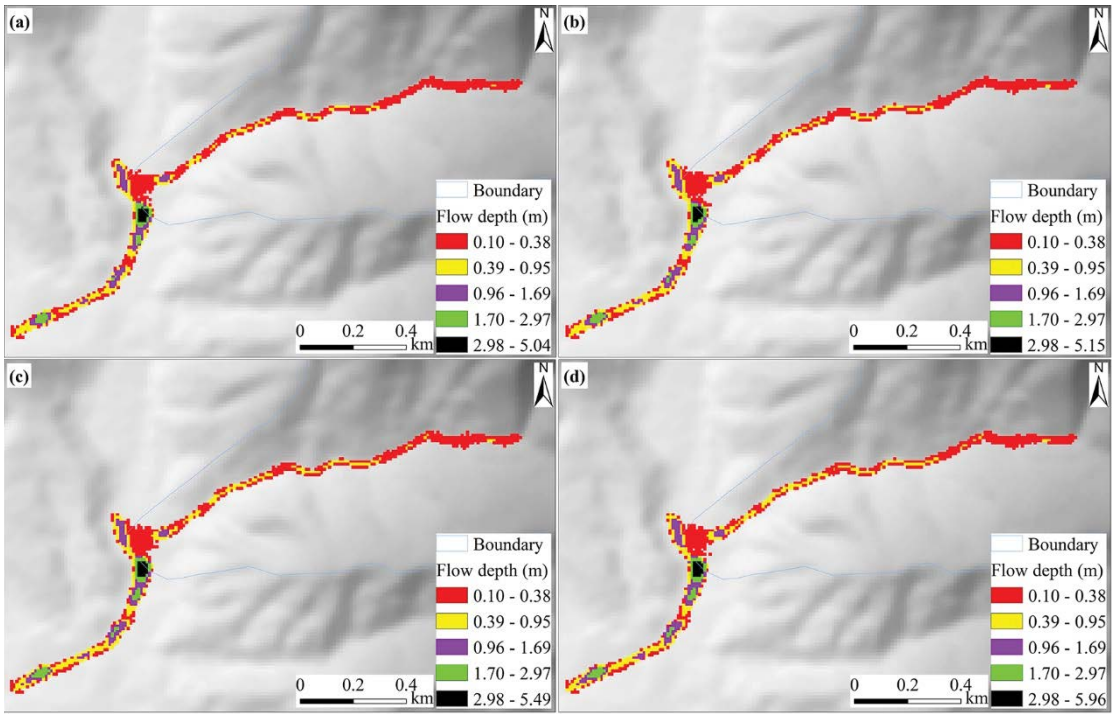

Fig. 7. Simulation results of flow depth for different return periods: (a) p = 10%, (b) p = 5%, (c) p = 2%, and (d) p = 1%.

and impact force were relatively high because higher velocity and impact force of debris flow will take abundant material downstream, so that the material cannot be left in the middle-up stream [58]. Eventually, the loose material is gradually deposited downstream and reaches a maximum flow depth. However, the lowest value is distributed upstream, which conforms to the actual debris flow. The maximum value of flow depth was 5.04, 5.15, 5.49 and 5.96 m under different RRP, respectively (Table 4). The maximum depth value gradually increased with increasing RRP; therefore, the increase in amplitude was the largest when the RRP was between 50 and 100 years, and the proportion of the increase in amplitude was 7.83%. With values of - 2.18% and - 6.60% when RRP ranged from 10 to 500 years. The increase in the

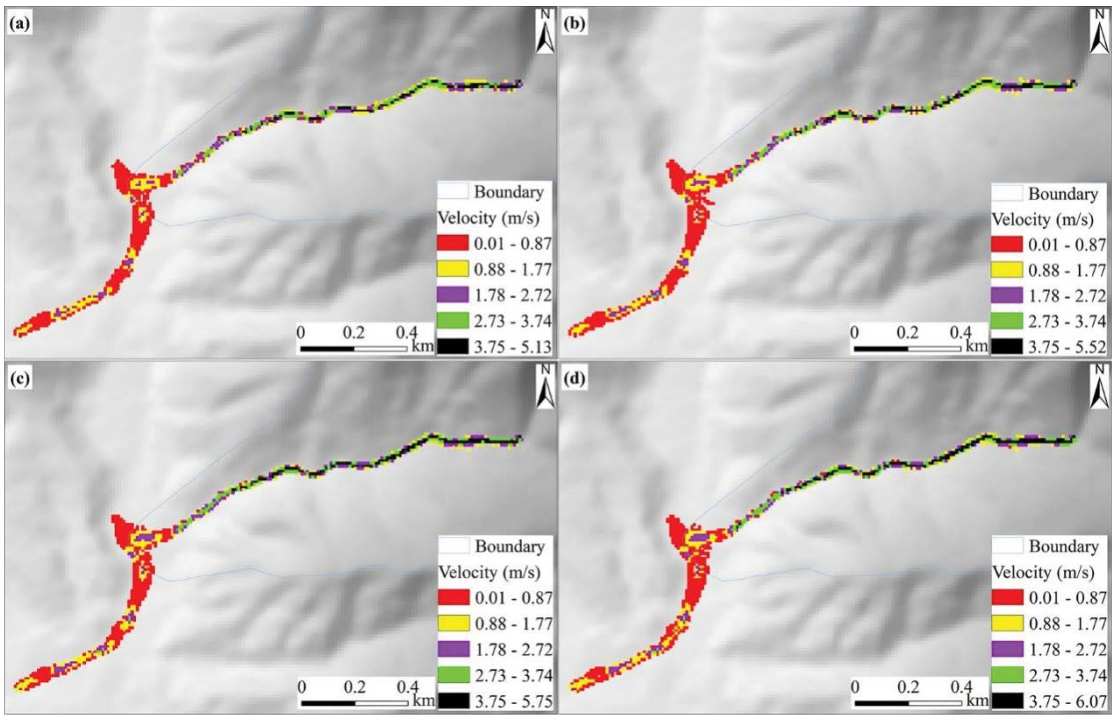

Fig. 8. Simulation results of velocity for different return periods: (a) p = 10%, (b) p = 5%, (c) p = 2%, and (d) p = 1%.

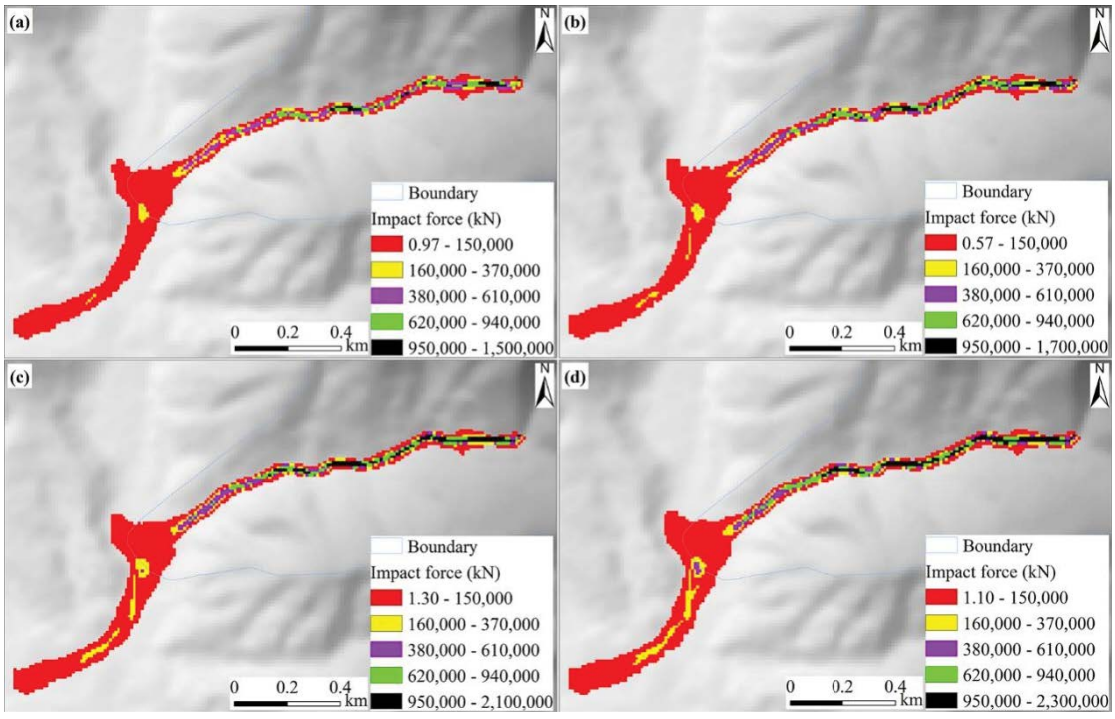

Fig. 9. Simulation results of impact force for different return periods: (a) p = 10%, (b) p = 5%, (c) p = 2%, and (d) p = 1%.

flow depth was obviously correlated with RRP. Generally, loose materials (i.e., landslide, collapse) may be increased due to gradual increase in rainfall, so that abundant sediment was left in the downstream section [59,60].

4.2.2. Velocity

The velocity generally decreased from the middle-up stream to the downstream under different RRP (Fig. 8), and this result was similar to the process of energy storage,

Table 4
Characteristics of debris flow for different rainfall periods

Maximum value \ RRP	p = 10%	p = 5%	p = 2%	p = 1%
Maximum flow depth (m)	5.04	5.15	5.49	5.96
Maximum velocity (m/s)	5.13	5.52	5.96	6.07
Maximum impact force (kN)	1,466,800	1,727,702	2,064,777	2,310,948

enablement, and consumption of physical tests [29,49]. The highest velocity of debris flow appeared in the middle section of the watershed channel (Fig. 8), which may be correlated to terrain changes. The maximum values of velocity were 5.13, 5.52, 5.96 and 6.07 m/s under each RRP, respectively (Table 4). The maximum value gradually increased with increasing rainfall return periods. Therefore, the increase in amplitude was the largest when the RRP was between 10 and 20 years, and the proportion of increase amplitude was 7.60%. With values of - 4.35% and - 5.38%, when the RRP ranged from 20 to 100 years. These amplitudes of velocity change may be related to the amount of loose material in the watershed channel because a lower bed friction was generated by less loose material in a certain time, which led to a higher velocity [61,62].

4.2.3. Impact force

The distribution of the impact force was obtained through numerical simulation under RRP of 10, 20, 50, and 100 years, and the impact force gradually decreased from the middle-up stream to the downstream (Fig. 9). The impact force was ordinarily high when the velocity was relatively high and the location of the maximum value was similar to that of the maximum velocity. The maximum value was distributed in the middle of the watershed channel, where several landslides occurred on both sides of the channel because potential energy was converted into kinetic energy in the process of landslide failure. Thus, the impact force rapidly increased in a short time [29,61,63]. The highest values of impact force were 1,466,800; 1,727,702; 2,064,777 and 2,310,948 kN under different RRP, respectively. The maximum depth value significantly increased with increasing RRP, and the increase amplitudes were 17.79%, 19.51%, and 11.92% when the RRP ranged from 10 to 100 years. Therefore, the amplitude of variation was largest when the RRP was between 20 and 50 years. The lowest impact force value is located in the Beiyu River.

From the above analysis, the impact of debris flow reached a maximum in the middle of the watershed channel, and the minimum impact was situated in the Beiyu River. On the other hand, with respect to the distribution of debris flow characteristics, the loose material of the middle-up stream will be rapidly removed from the middle-up stream downstream when the velocity and impact force are relatively high. However, the loose material will be left downstream when the impact force and velocity are gradually decreased, so that abundant material is deposited. Therefore, the numerical simulation results can better reproduce debris flow movement and sedimentation processes.

4.3. Hazard assessment

4.3.1. Intensity assessment

The intensity value can be obtained based on the division criteria of intensity under different RRP. The spatial analysis technology of ArcGIS software was applied to divide the intensity class (Fig. 10), and the area and its proportion of intensity were calculated (Table 5). The spatial distribution of intensity classed was similar under RRP. However, there was a slight difference in the local area, such as in the downstream area, particularly near the Beiyu River, where the intensity gradually increased with increasing RRP.

The high-intensity class was mostly distributed in the middle-up stream channel when RRP was 10 years, and it was further observed in the Beiyu River. On the other hand, its proportion was accounted for approximately 26.13% of the total area. With respect to the RRP between 20 and 100 years, the high class was situated in the middle-up stream and Beiyu River, and the area of the high-intensity class gradually increased with increasing RRP (particularly near the Beiyu River area), seriously threatening the life and property (i.e., residents, roads, and railways) of the downstream watershed. Their proportions were 26.13%, 33.74%, 40.32%, and 44.13%, respectively, indicating that several areas in the study area were prone to debris flow disasters when RRP exceeded 50 years, which is consistent with other studies [24,49]. The increase in amplitude was the largest when the RRP was between 10 and 20 years, and the proportion of increase amplitude was 7.61%, with values of - 6.57% and - 3.81% when the RRP ranged from 20 to 100 years. The low- and medium-intensity areas gradually decreased with increasing RRP. Therefore, the low-intensity class was primarily situated downstream of the watershed channel, such as in the Beiyu River area, because the velocity and impact force were relatively small. The proportions of low-intensity classes were 35.28%, 32.16%, 28.34%, and 26.06% when the RRP was 10, 20, 50 and 100 years, respectively. For the medium-intensity class, the proportions were 38.59%, 34.10%, 31.35%, and 29.81% for each corresponding RRP, respectively, and they were mostly distributed around the high-intensity area.

4.3.2. Hazard assessment result

The hazard value was calculated based on the matrix method and hazard mapping was performed using ArcGIS software as per the actual situation in the study area (Fig. 11). Moreover, the proportion of different hazard areas was accounted for in (Table 6).

Their area proportions accounted for 28.99%, 35.48%, and 35.53% of the total area in the low, medium, and high

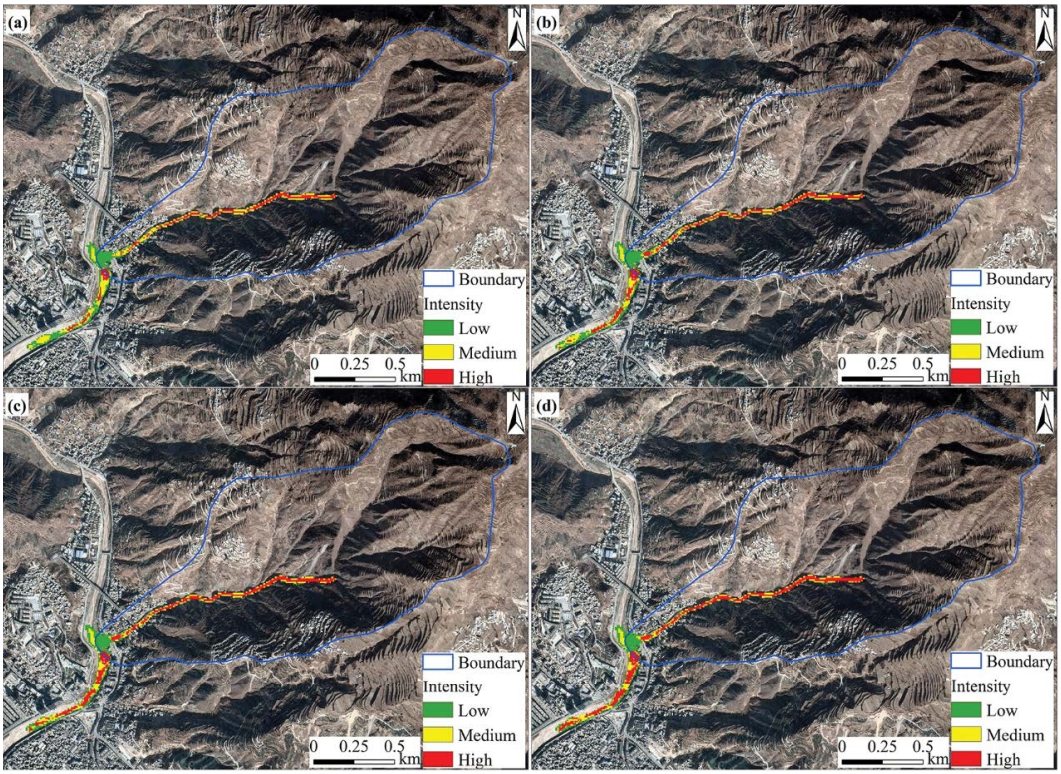

Fig. 10. Simulation result of debris flow intensity zoning in study area: (a) p = 10%, (b) p = 5%, (c) p = 2%, and (d) p = 1%.

Table 5
Area and its proportion of intensity under different rainfall return periods

Intensity \ RRP	p = 10%	p = 5%	p = 2%	p = 1%	p = 10%	p = 5%	p = 2%	p = 1%
	Area (104 m^2)				Area proportion (%)			
Low	3.05	2.86	2.59	2.40	35.28	32.16	28.34	26.06
Medium	3.33	3.03	2.86	2.74	38.59	34.10	31.34	29.81
High	2.26	3.00	3.68	4.06	26.13	33.74	40.32	44.13

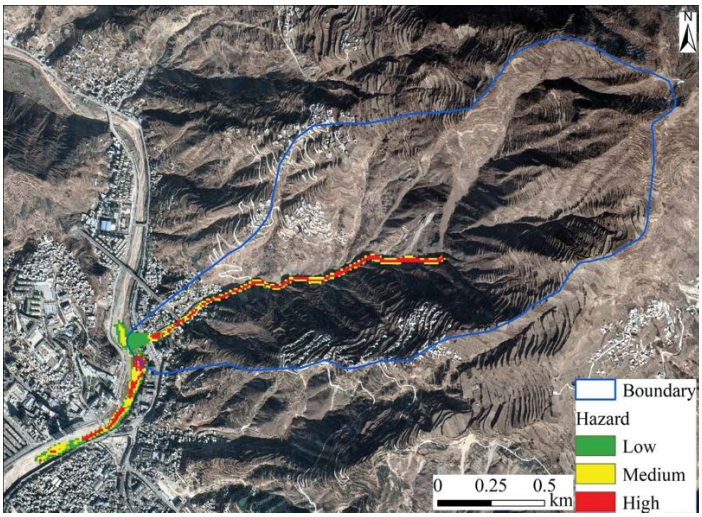

Fig. 11. Distribution of different debris flow hazard classes.

Table 6
Area statistical result and its proportion of different hazard classes

Hazard classes	Area (104 m^2)	Area proportion (%)
Low	2.43	28.99
Medium	2.97	35.48
High	2.98	35.53

hazard classes, respectively, indicating that there is a relatively high probability of debris flow occurrence, and this result was generally similar to that of other studies [24,49]. A large number of loose materials existed in the middle-up of watershed channel (Fig. 2 and 3). Furthermore, the elevation difference of terrain was relatively large, and these conditions will eventually contribute to the occurrence of debris flow disaster. Therefore, the middle-up of watershed channel area mostly belonged to high hazard class. Meanwhile, a high hazard was also present downstream of the watershed, in the Beiyu River and around the residents' area. In the event of extreme rainfall, the life and property of the downstream watershed were significantly influenced. Additionally, if abundant sedimentation is left in the Beiyu River, it may block the river, threatening serious disaster in Longnan. The low-hazard area was situated downstream of the channel, particularly in the Beiyu River, and it demonstrated the frequency of a potentially low damaging phenomenon. However, a large number of people and infrastructure (i.e., roads, railways, and hospitals) are distributed downstream of the watershed, and a smaller debris flow disaster may cause a greater loss of life and property. The medium hazard area was around the high hazard area in the middle of the watershed channel, indicating that these areas are prone to debris flow disasters. Downstream of the watershed, the medium hazard class was located between the high and low classes.

From the above analysis, the proportion of high-medium hazard areas was more than 70%, and it was demonstrated that geohazards, such as landslides and debris flow may occur very easily in the present study area, causing a series of significant loss of life and property, particularly downstream of the watershed. Therefore, various disaster prevention and mitigation measures need to be implemented. Xiong et al. [9] suggested that channel engineering measures and ecological measures should be sufficiently combined to minimize debris flow damage in the high mountains of the Bailong River, and this idea has been well implemented in the Goulinping Gully of the Bailong River. With respect to the present study area, the debris flow characteristics were generally similar to those of the Goulinping Gully; however, their distances were relatively close. The ecological measures should be positively conducted in the middle-up stream of the catchment; with assisted engineering measures. The check dam was built downstream, which is not a reasonable measure [8,64]. Moreover, in densely populated areas, drainage channels should be used to reduce debris flow hazards. If these measures can be actively implemented, the desire for sustainable development will be realized.

5. Conclusions

In recent years, landslides generally increased with an increase in human activities (i.e., road building and railway construction) in the Qingshui Gully.

The flow depth generally increased from middle-up stream to downstream when RRP ranged from 10 to 100 years. The maximum value of flow depth was 5.04, 5.15, 5.49 and 5.46 m under different RRP, respectively. The velocity generally decreased from the middle-up stream to the downstream, and the maximum values of the velocity were 5.13, 5.52, 5.96 and 6.07 m/s. The impact force gradually decreased from the middle-up stream to the downstream, and the highest values of the impact force were 1,466,800; 1,727,702; 2,064,777 and 2,310,948 kN. Additionally, the simulation result of the threatened range was generally consistent with the actual result of the debris flow disaster on August 12, 2010, demonstrating that the results of the numerical simulation were highly reliable.

The spatial distribution of different intensity classes was similar under RRP ranging from 10 to 100 years in a certain, and the high-medium intensity area was primarily distributed in the middle-up stream of the study area, while the low-intensity area was located downstream. The proportions of the high-intensity area were 26.13%, 33.74%, 40.32%, and 44.13% under different RRP, respectively. The percentages of medium areas were 38.59%, 34.10%, 31.34%, and 29.81%, respectively. The low-intensity areas accounted for 35.28%, 32.16%, 28.34%, and 26.06%, respectively. The middle-up watershed channel area mostly belonged to the high hazard class, and it also existed downstream of the watershed, such as in the Beiyu River and around the residential area. The low-hazard area was situated downstream of the channel, particularly in the Beiyu River. The medium hazard class was located between the high and low classes. These proportions accounted for 28.99%, 35.48%, and 35.53% of the total area with low, medium, and high hazard areas, respectively.

Engineering measures combined with ecological measures are a better approach to minimize debris flow damage at the debris flow watershed characteristic with the dry hot river valley in the high mountains.

Author contributions

Conceptualization, Heping Shu; Formal analysis, Peng Zhang and Xingrong Liu; Funding acquisition, Heping Shu; Investigation, Peng Zhang and Xingrong Liu; Methodology, Peng Zhang and Xingrong Liu; Project administration, Heping Shu; Software, Peng Zhang; Visualization, Xingrong Liu and Heping Shu; Writing – original draft, Peng Zhang; Writing – review & editing, Xingrong Liu and Heping Shu.

Acknowledgments

This work is supported by the Hubei Key Laboratory of Disaster Prevention and Mitigation (China Three Gorges University) (No. 2021KJZ05), Doctoral Foundation of Gansu Agricultural University (No. GAU-KYQD-2022-04), Water Resources Department Project of Gansu Province (Nos. 23GSLK082 and 23GSLK091), Gansu Province 2021

Key Talent Project (No. 2021RCXM066), Gansu Academy of Sciences Applied Research and Development Project (No. 2021JK-07) and Fundamental Research Funds for the Central Universities (No. lzujbky-2022-pd01).

References

[1] P.M. Santi, K. Hewitt, D.F. VanDine, E. Barillas Cruz, Debris-flow impact, vulnerability, and response, Nat. Hazards, 56 (2011) 371–402.
[2] P. Kattel, J. Kafle, J.-T. Fischer, M. Mergili, B.M. Tuladhar, S.P. Pudasaini, Interaction of two-phase debris flow with obstacles, Eng. Geol., 242 (2018) 197–217.
[3] H. Luo, L. Zhang, H. Wang, J. He, Multi-hazard vulnerability of buildings to debris flows, Eng. Geol., 279 (2020) 105859, doi: 10.1016/j.enggeo.2020.105859.
[4] W. Li, J. Zhu, S. Pirasteh, Q. Zhu, L. Fu, J. Wu, Y. Hu, Y. Dehbi, Investigations of disaster information representation from a geospatial perspective: progress, challenges and recommendations, Trans. GIS, 26 (2022) 1376–1398.
[5] Z. Zhang, M. Li, J. Wang, Z. Yin, Y. Yang, X. Xun, Q. Wu, A calculation model for the spatial distribution and reserves of ground ice - a case study of the Northeast China permafrost area, Eng. Geol., 315 (2023) 107022, doi: 10.1016/j.enggeo.2023.107022.
[6] H. Shu, M. Hürlimann, R. Molowny-Horas, M. González, J. Pinyol, C. Abancó, J. Ma, Relation between land cover and landslide susceptibility in Val d'Aran, Pyrenees (Spain): historical aspects, present situation and forward prediction, Sci. Total Environ., 693 (2019) 133557, doi: 10.1016/j.scitotenv.2019.07.363.
[7] M. Jakob, P. Friele, Frequency and magnitude of debris flows on Cheekye River, British Columbia, Geomorphology, 114 (2010) 382–395.
[8] P. Cui, G.G.D. Zhou, X.H. Zhu, J.Q. Zhang, Scale amplification of natural debris flows caused by cascading landslide dam failures, Geomorphology, 182 (2013) 173–189.
[9] M. Xiong, X. Meng, S. Wang, P. Guo, Y. Li, G. Chen, F. Qing, Z. Cui, Y. Zhao, Effectiveness of debris flow mitigation strategies in mountainous regions, Prog. Phys. Geogr., 40 (2016) 768–793.
[10] Y. Chong, G. Chen, X. Meng, Y. Yang, W. Shi, S. Bian, Y. Zhang, D. Yue, Quantitative analysis of artificial dam failure effects on debris flows – a case study of the Zhouqu '8.8' debris flow in northwestern China, Sci. Total Environ., 792 (2021) 148439, doi: 10.1016/j.scitotenv.2021.148439.
[11] M. Hürlimann, D. Rickenmann, V. Medina, A. Bateman, Evaluation of approaches to calculate debris-flow parameters for hazard assessment, Eng. Geol., 102 (2008) 152–163.
[12] G.G. Chevalier, V. Medina, M. Hürlimann, A. Bateman, Debris-flow susceptibility analysis using fluvio-morphological parameters and data mining: application to the Central-Eastern Pyrenees, Nat. Hazards, 67 (2013) 213–238.
[13] L. Yu, C. Peng, A.D. Regmi, V. Murray, A. Pasuto, G. Titti, M. Shafique, T. Priyadarshana D.G., An international program on Silk Road Disaster Risk Reduction–a Belt and Road initiative (2016–2020), J. Mountain Sci., 15 (2018) 1383–1396.
[14] C. Scheidl, M. Chiari, R. Kaitna, M. Müllegger, A. Krawtschuk, T. Zimmermann, D. Proske, Analysing debris-flow impact models, based on a small-scale modelling approach, Surv. Geophys., 34 (2013) 121–140.
[15] H. Shu, J. Ma, J. Guo, S. Qi, Z. Guo, P. Zhang, Effects of rainfall on surface environment and morphological characteristics in the Loess Plateau, Environ. Sci. Pollut. Res., 27 (2020) 37455–37467.
[16] H. Shu, J. Ma, S. Qi, P. Chen, Z.Z. Guo, P. Zhang, Experimental results of the impact pressure of debris flows in loess regions, Nat. Hazards, 103 (2020) 3329–3356.
[17] R.M. Iverson, M.E. Reid, M. Logan, R.G. LaHusen, J.W. Godt, J.P. Griswold, Positive feedback and momentum growth during debris-flow entrainment of wet bed sediment, Nat. Geosci., 4 (2011) 116–121.
[18] L. Bugnion, B.W. McArdell, P. Bartelt, C. Wendeler, Measurements of hillslope debris flow impact pressure on obstacles, Landslides, 9 (2012) 179–187.
[19] T. de Haas, A.L. Densmore, M. Stoffel, H. Suwa, F. Imaizumi, J.A. Ballesteros-Cánovas, T. Wasklewicz, 2018. Avulsions and the spatio-temporal evolution of debris-flow fans, Earth Sci. Rev., 177 (2018) 53–75.
[20] C. Scheip, K. Wegmann, Insights on the growth and mobility of debris flows from repeat high-resolution lidar, Landslides, 19 (2022) 1297–1319.
[21] F. Gentile, T. Bisantino, G.T. Liuzzi, Debris-flow risk analysis in south Gargano watersheds (Southern-Italy), Nat. Hazards, 44 (2008) 1–17.
[22] H. Raetzo, O. Lateltin, D. Bollinger, J. Tripet, Hazard assessment in Switzerland – Codes of Practice for mass movements, Bull. Eng. Geol. Environ., 61 (2002) 263–268.
[23] W.-j. Liang, D.-f. Zhuang, D. Jiang, J.-j. Pan, H.-y. Ren, Assessment of debris flow hazards using a Bayesian Network, Geomorphology, 171–172 (2012) 94–100.
[24] H. Shu, J. Ma, P. Zhang, H. Yu, S. Ren, S. Qi, H. Yang, Debris-flow risk assessment: from catchment to regional scale: a case study from Southern Gansu Province, China, Ekoloji, 28 (2019) 2319–2333.
[25] S. Zhang, A comprehensive approach to the observation and prevention of debris flows in China, Nat. Hazards, 7 (1993) 1–23.
[26] B.W. McArdell, P. Bartelt, J. Kowalski, Field observations of basal forces and fluid pore pressure in a debris flow, Geophys. Res. Lett., 34 (2007), doi: 10.1029/2006GL029183.
[27] T. Takahashi, A review of Japanese debris flow research, Int. J. Erosion Control Eng., 2 (2013) 1–14.
[28] J.-b. Tang, K.-h. Hu, A debris-flow impact pressure model combining material characteristics and flow dynamic parameters, J. Mountain Sci., 15 (2018) 2721–2729.
[29] H. Shu, J. Ma, H. Yu, M. Hürlimann, P. Zhang, F. Liu, S. Qi, Effect of density and total weight on flow depth, velocity, and stresses in loess debris flows, Water, 10 (2018) 1784, doi: 10.3390/w10121784.
[30] R.K. Dash, D.P. Kanungo, J.P. Malet, Runout modelling and hazard assessment of Tangni debris flow in Garhwal Himalayas, India, Environ. Earth Sci., 80 (2021) 338, doi: 10.1007/s12665-021-09637-z.
[31] H. Cheng, Y. Huang, W. Zhang, Q. Xu, Physical process-based runout modeling and hazard assessment of catastrophic debris flow using SPH incorporated with ArcGIS: a case study of the Hongchun gully, Catena, 212 (2022) 106052, doi: 10.1016/j.catena.2022.106052.
[32] P. Shen, L. Zhang, H. Chen, R. Fan, EDDA 2.0: integrated simulation of debris flow initiation and dynamics considering two initiation mechanisms, Geosci. Model Dev., 11 (2018) 2841–2856.
[33] J.S. O'Brien, P.J. Julien, W.T. Fullerton, Two-dimensional water flood and mudflow simulation, J. Hydraul. Eng., 119 (1993) 244–261.
[34] O. Hungr, S. McDougall, Two numerical models for landslide dynamic analysis, Comput. Geosci., 35 (2009) 978–992.
[35] A. von Boetticher, J.M. Turowski, B.W. McArdell, D. Rickenmann, M. Hürlimann, C. Scheidl, J.W. Kirchner, DebrisInterMixing-2.3: a finite volume solver for three-dimensional debris-flow simulations with two calibration parameters – Part 2: model validation with experiments, Geosci. Model Dev., 10 (2017) 3963–3978.
[36] P. Zhang, J. Ma, H. Shu, T. Han, Y. Zhang, Simulating debris flow deposition using a two-dimensional finite model and Soil Conservation Service-curve number approach for Hanlin Gully of southern Gansu (China), Environ. Earth Sci., 73 (2015) 6417–6426.
[37] P. Bertolo, G.F. Wieczorek, Calibration of numerical models for small debris flows in Yosemite Valley, California, USA, Nat. Hazards Earth Syst. Sci., 5 (2005) 993–1001.
[38] C.-Y. Chen, Q. Wang, Debris flow-induced topographic changes: effects of recurrent debris flow initiation, Environ. Monit. Assess., 189 (2017) 449, doi: 10.1007/s10661-017-6169-y.

[39] Z. Deng, J. Liu, L. Guo, J. Li, J. Li, Y. Jia, Pure risk premium rating of debris flows based on a dynamic run-out model: a case study in Anzhou, China, Nat. Hazards, 106 (2021) 235–253.
[40] H. Shu, S. Qi, N. Ning, J. Ma, P. Zhang, Risk assessment of debris flow disaster: a case study of Wudu District in the south of Gansu Province China, J. Nat. Disasters, 25 (2016) 34–41 (in Chinese).
[41] S. Bai, J. Wang, B. Thiebes, C. Cheng, Y. Yang, Analysis of the relationship of landslide occurrence with rainfall: a case study of Wudu County, China, Arabian J. Geosci., 7 (2014) 1277–1285.
[42] S.B. Bai, J. Wang, F.Y. Zhang, A. Pozdnoukhov, M. Kanevski, Prediction of Landslide Susceptibility Using Logistic Regression: A Case Study in Bailongjiang River Basin, China, J. Ma, Y. Yin, J. Yu, S.G. Zhou, Eds., Proceedings of the Fifth International Conference on Fuzzy Systems and Knowledge Discovery (FSKD 2008), Vol. 4, IEEE, Jinan, China, 2008, pp. 647–651.
[43] J.S. O'Brien, FLO-2D User's Manual, Non-published Reference Manual, Version 99.2, FLO-2D Software, Inc., Nutrioso, Arizona, US, 1999.
[44] J.S. O'Brien, FLO-2D User's Manual, Version 2006.01, FLO-2D Software, Inc., Nutrioso, Arizona, US, 2006.
[45] P. Canuti, N. Casagli, F. Catani, G. Falorni, Modeling of the Guagua Pichincha volcano (Ecuador) lahars, Phys. Chem. Earth Parts A/B/C, 27 (2002) 1587–1599.
[46] C. Calligaris, M.A. Boniello, L. Zini, Debris flow modelling in Julian Alps using FLO-2D, WIT Trans. Eng. Sci., 60 (2008) 81–88.
[47] J. Ma, X. Wang, P. Zhang, S. Qi, Geological Hazard and Risk Analysis of Landslide and Debris Flow in Bailong River Basin, Lanzhou University Press, Lanzhou, 2015 (in Chinese).
[48] P. Zhang, J.Z. Ma, H.P. Shu, G. Wang, Numerical simulation of erosion and deposition debris flow based on FLO-2D Model, J. Lanzhou Univ. (Nat. Sci.), 50 (2014) 363–375 (in Chinese).
[49] P. Zhang, Hazard Assessment and Predicting Method of Debris Flow of Small Catchments in Earthquake-Affected Regions, Ph.D. Theses, Lanzhou University, Lanzhou, 2015 (in Chinese).
[50] D.A. Woolhiser, Simulation of Unsteady Overland Flow, K. Mahmood, V. Yevjevich, Eds., Unsteady Flow in Open Channels, Water Resources Publications, Fort Collins, 1975, pp. 485–508.
[51] L.H. Xiong, S.L. Guo, P. Liu, Reliability study on design floods derived from the Pearson TypeIII distribution, Int. J. Hydroelectric Energy, 20 (2002) 48–50 (in Chinese).
[52] R. Fell, J. Corominas, C. Bonnard, L. Cascini, E. Leroi, W.Z. Savage, Guidelines for landslide susceptibility, hazard and risk zoning for land use planning, Eng. Geol., 102 (2008) 85–98.
[53] P. Aleotti, G. Polloni, Two-dimensional Model of the 1998 Sarno Debris Flows (Italy): Preliminary Results, D. Rickenmann, C.L. Chen, Eds., Third International Conference on Debris-flow Hazards Mitigation: Mechanics, Prediction, and Assessment, Millpress, Rotterdam, 2003, pp. 553–563.
[54] D. Rickenmann, Hangmuren und Gefahrenbeurteilung. Kurzbericht für dasBundesamt für Wasser und Geologie, Unpublished Report, Universität für Bodenkultur, Wien, und Eidg. Forschungsanstalt WSL, Birmensdorf, 2005, 18 p.
[55] S.C. Chen, C.Y. Wu, B.T. Huang, The efficiency of a risk reduction program for debris-flow disasters – a case study of the Songhe community in Taiwan, Nat. Hazards Earth Syst. Sci., 10 (2010) 1591–1603.
[56] D.J. Varnes, Hazard Zonation: A Review of Principal and Practice, The United Nations Educational, Scientific, Cultural Organization (UNESCO), Paris, 1984, 63 p.
[57] BUWAL, Berücksichtigung der Hochwassergefahren bei raumwirksamen Tätigkeiten, Empfehlungen. Bundesamt für Umwelt Wald und Landschaft, Switzerland, Berne, 1997, 42 pp.
[58] M. Jakob, Debris-flow Hazard Analysis, In: Debris-flow Hazards and Related Phenomena, Springer, Berlin, 2005, pp. 411–443.
[59] V. D'Agostino, M. Cesca, L. Marchi, Field and laboratory investigations of runout distances of debris flows in the Dolomites (Eastern Italian Alps), Geomorphology, 115 (2010) 294–304.
[60] M. Hürlimann, B.W. McArdell, C. Rickli, Field and laboratory analysis of the runout characteristics of hillslope debris flows in Switzerland, Geomorphology, 20 (2015) 20–32.
[61] R.M. Iverson, The Physics of Debris Flows, Rev. Geophys., 35 (1997) 245–296.
[62] B. Turnbull, E.T. Bowman, J.N. McElwaine, Debris flows: experiments and modelling, C.R. Phys., 16 (2015) 86–96.
[63] T. de Haas, L. Braat, J.R.F.W. Leuven, I.R. Lokhorst, M.G. Kleinhans, Effects of debris flow composition on runout, depositional mechanisms, and deposit morphology in laboratory experiments, J. Geophys. Res.: Earth Surf., 120 (2015) 1949–1972.
[64] T.A. Dijkstra, J. Wasowski, M.G. Winter, X.M. Meng, Introduction to geohazards of central China, Q. J. Eng. Geol. Hydrogeol., 47 (2014) 195–199.